

1. Department of Research

As an inter-university research institute, the National Institute for Fusion Science (NIFS) is required to continue to conduct cutting-edge academic research that supports the development of fusion science as an interdisciplinary collaboration with the active participation of researchers and students from a wide range of fields. To strengthen and expand collaboration between NIFS and universities through interdisciplinary research, a new “Unit System” was established over two years of discussion and implemented in FY2023.

In FY2024 there were new appointments that included an associate professor, two cross-appointed researchers, five specially appointed researchers, and four visiting professors from abroad. Additionally, a total of 246 Unit members, which included 125 external members of the Unit Research Strategy Committees, conducted research activities alongside 1,649 co-researchers from domestic and international research institutions. In the second year since the Unit system was implemented, it is becoming well-established, and the results of the reform are starting to show, such as a 30% increase in the number of research papers published.

To foster opportunities for research collaboration, we organize open seminars at different levels. Each Unit has planned and conducted a total of fifty-nine seminars, while the Department of Research and the Institute has hosted eight additional seminars. All these seminars are accessible to the research community and the public through our website (<https://www.nifs.ac.jp/about/reio/all/>) and mailing list. Participants can join both online and in person. The Units have actively communicated their research activities to the public by issuing 13 press-releases, and using EurekaAlert! for international information dissemination. Additionally, the Units and the LHD project have created a website (<https://www-lhd.nifs.ac.jp/pub/Science.html>) that offers easy-to-understand summaries of scientific papers, effectively communicating the research activities.

The findings from the Units’ research in FY2024 were reported during the Unit Research Results Reporting Meeting, held from May 28–29, 2025. The presentations and meeting minutes can be accessed on the following website (<https://unit.nifs.ac.jp/research/archives/articles/articles-9271>). A detailed overview of the Units’ research results in FY2024 is presented in the following pages.

(R. Sakamoto)



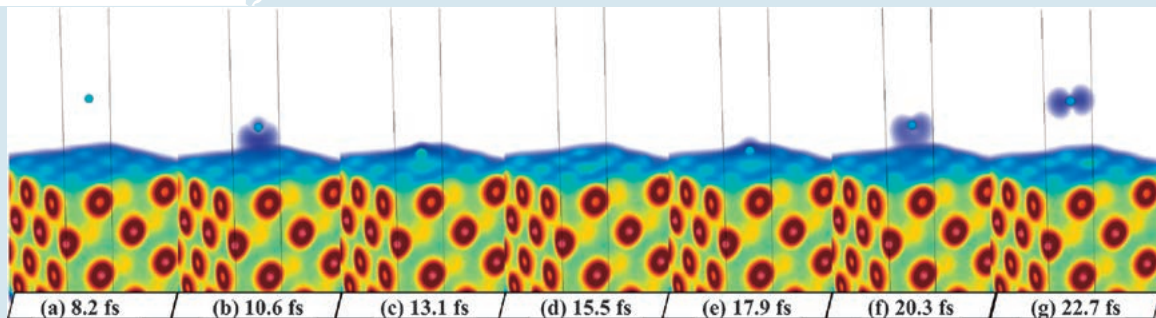
Meta-hierarchy Dynamics Unit

Highlight

Helium Ion Neutralization on Tungsten: An Ehrenfest Molecular Dynamics Approach

Plasma-material interactions (PMI) encompass a broad spectrum of physical phenomena. Among these, we previously examined within the context of meta-hierarchy dynamics is gradual surface morphology evolution, such as fuzz formation, induced by long-time exposure to helium plasma. Another interpretation of PMI within meta-hierarchy dynamics is the neutralization of ions, where incident ions capture electrons from the solid surface. Unlike conventional models treating plasma particles as classical mechanics, this process requires a quantum-mechanical description of electron transitions from the surface.

Historically, PMI simulation has been performed using binary collision approximation (BCA) and molecular dynamics (MD), both of which are fundamentally classical approaches. Even density functional theory (DFT), when applied within the Born–Oppenheimer approximation, fails to capture the quantum dynamics of the electron transfer required for ion neutralization. To address this, we developed the QUMASUN code, which solves time-dependent Kohn–Sham equations for electronic quantum dynamics and Newton’s equation for nuclei, following Ehrenfest molecular dynamics formalism. The figure illustrates the electron capture of an incident He^{2+} ion on a tungsten surface. Notably, the reflected He exists as a superposition of He^{2+} , He^+ , and neutral He states. This highlights the potential of PMI phenomena, when viewed through the lens of meta-hierarchical dynamics, to serve as a testbed for investigating coupled classical and quantum dynamical systems.



(A.M. Ito (NIFS, SOKENDAI), Y. Toda (SOKENDAI) and A. Takayama (NIFS, SOKENDAI))

Highlight

Beam divergence degradation with the RF field at the beam extraction region

The convergence of negative ion beams is a critical issue in the development of the ITER neutral beam injector (NBI). The beam divergence angle produced by the RF-driven negative ion source currently remains nearly twice as large as the specification required by the ITER design. To address this discrepancy, we conducted an experimental investigation using the NIFS Negative Ion Beam Test Stand (NIFS-NBTS). Our study identified a direct response of the beam divergence to the externally applied RF field in the beam extraction region.

Figure 1 presents a schematic diagram of the experimental setup, and a typical waveform is shown in Figure 2. Notably, oscillations in the beam width were observed at a frequency matching that of the applied RF field. This observation strongly suggests that RF perturbations in the extraction region can degrade beam convergence.

A detailed analysis revealed that the oscillatory behavior of the beam divergence angle can be understood in terms of its dependence on beam perveance. Furthermore, we identified optimal operational conditions under which the influence of RF perturbations on beam convergence is minimized.

These findings contribute not only to the improvement of beam convergence in ITER NBI systems, but also to the broader application of negative ion beams in areas such as medical accelerator facilities and materials science.

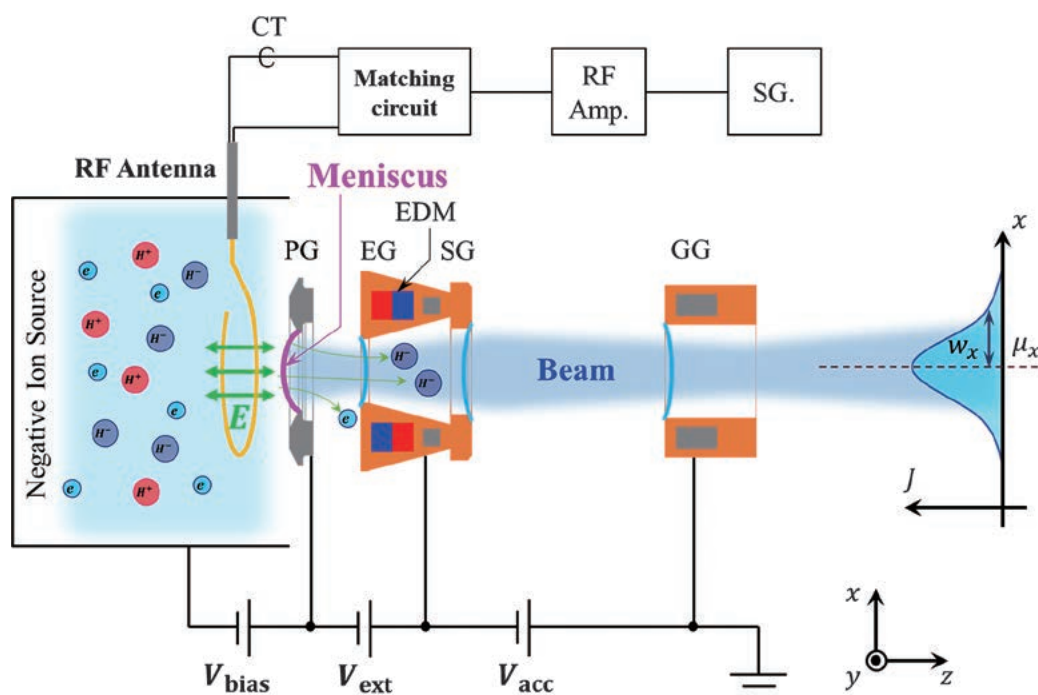


Fig. 1 Schematic of the present experimental setup. The beam width is evaluated by the Gaussian fitting of the beam profile measured at 0.92 m downstream of the ion source.

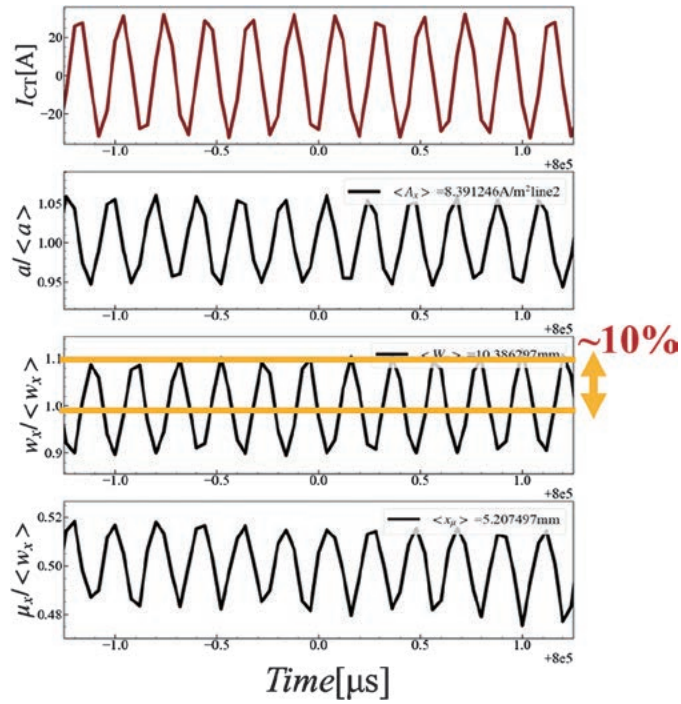


Fig. 2 A typical waveform of (top) externally driven RF current to the antenna, (second) the peak current density, (third) the beam width, and (bottom) the position of the beam center obtained by the Gaussian fitting.

(K. Nagaoka)

Highlight

Reconstruction of electron velocity distribution function and Gibbs entropy from electron cyclotron emission spectrum in optically thin plasmas

The Kolmogorov theory of energy cascades in neutral three-dimensional turbulence—characterized by the $-5/3$ power law in the wavenumber spectrum of energy—is an exemplary model illustrating the universality of nonlinear, strongly correlated systems.

In magnetized plasma turbulence, correlations arise not only in configuration space but also between configuration and velocity space. Gyrokinetic theory predicts phase-space entropy cascades with scaling laws reflecting the universality of this turbulence. Our goal is to reveal such universal behavior at electron scales.

This year, we developed a method to obtain electron Gibbs entropy $-\int \delta f_e(v_\perp) \ln \delta f_e(v_\perp) dv_\perp$, where $\delta f_e(v_\perp)$ is the fluctuation of the electron velocity distribution function (EVDF), from the electron cyclotron emission (ECE) spectrum [1], and conducted an experimental validation using the LHD device, where v_\perp is the electron velocity perpendicular to the magnetic field.

We used the maximum entropy method (MEM) in velocity space with the Hankel transform (HT), converting v_\perp to ρ , the velocity-space wavenumber. Combined with spatial diagnostics, this method reconstructs entropy distribution in ω - ρ space, enabling analysis of entropy transport in magnetized plasmas.

Figure 1 shows (left) $\delta f_e(\omega, v_\perp)$ and (right) the entropy distribution $S(\omega, \rho)$ in ω - ρ space, reconstructed via the MEM-HT method from ECE spectra in an LHD plasma, where EVDF is perturbed by a 10 Hz-modulated neutral beam injection. Signatures of the perturbed EVDF and $S(\omega, \rho)$ are evident. In the next LHD experimental campaign, we plan to use this method to study entropy linked to electron-scale turbulence.

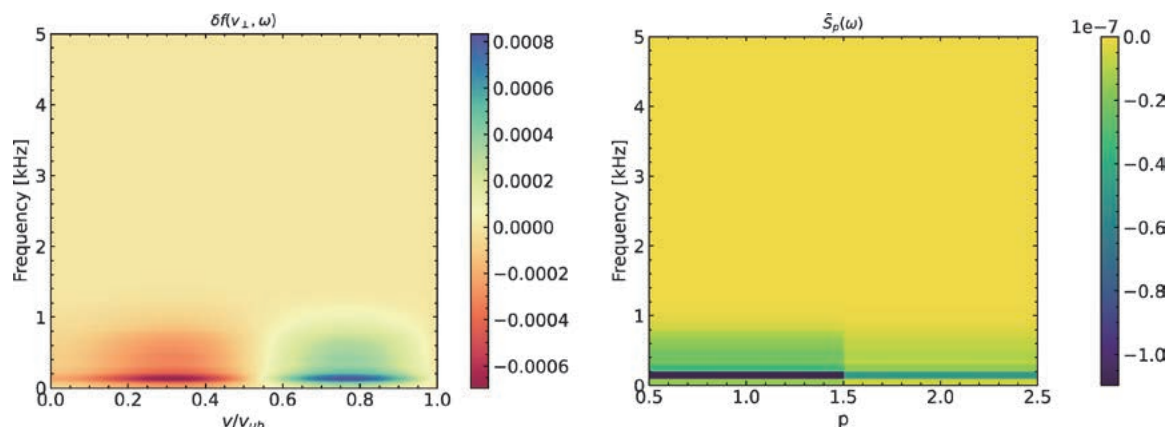


Fig. 1 (left) $\delta f_e(\omega, v_\perp)$ and (right) the entropy distribution $S(\omega, \rho)$, reconstructed using the MEM-HT method for the ECE spectrum measured in an LHD plasma in which external perturbations were applied to the EVDF by modulating the neutral beam injection at 10 Hz, where ω and ρ denote frequency and wave-number index in velocity space, respectively.

[1] Eiichirou Kawamori, Nucl. Fusion **65**, 026024 (2025).

Structure Formation and Sustainability Unit

Highlight

Development of synthetic diagnostics for energetic particle confinement study

Understanding energetic particle confinement is one of the key issues in achieving high-temperature and high-density plasma. To investigate energetic particle behavior in magnetically confined fusion plasma, information on energetic particle distribution is essential. To measure the energy and spatial profiles of energetic particles, an imaging neutral particle analyzer (INPA) for the Large Helical Device (LHD) has been developed as part of a Ph.D. program for a SOKENDAI student through international collaboration among NIFS, General Atomics (USA), and Mahasarakham University (Thailand) (Fig. 1 Left). The imaging neutral particle analyzer, originally developed in the USA, consists of an aperture, a stripping carbon foil, and a scintillator. Energetic neutrals, which escape from the plasma due to charge exchange reactions, pass through the aperture and are reionized by the stripping foil. The re-ionized energetic particles bombard the scintillator according to the charge-exchanged position and energy. We obtain the energy and spatial distribution of energetic neutrals to the INPA by measurement of the scintillation pattern by a fast camera. The imaging neutral particle analyzer in LHD was designed to have two apertures to measure energetic neutrals under both toroidal magnetic field conditions [1]. In high-temperature plasma discharges performed under relatively low-density conditions in LHD, this high-temperature state is often terminated by a magnetohydrodynamic instability, the energetic ion driven resistive interchange mode (EIC), excited by steep pressure gradients of helically trapped energetic ions. The INPA was used to investigate changes in the energetic ion distribution. We found that the distribution of energetic neutrals to the INPA changed due to the excitation of the EIC [2] (Fig. 1 Middle and Right). Advances in synthetic diagnostics further enhance the understanding of energetic particle confinement as well as making a significant contribution to developing human resources for the future.

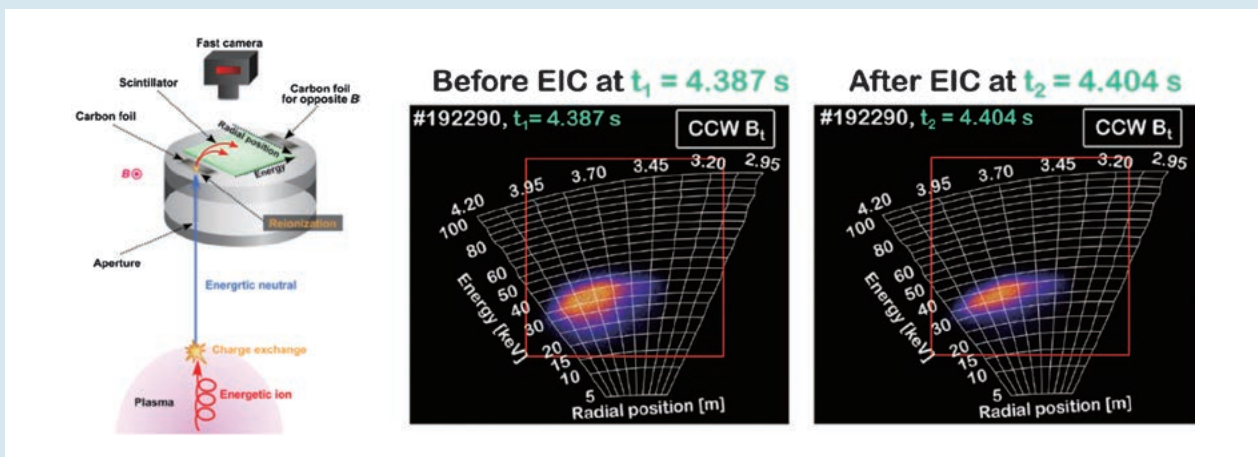


Fig. 1 (left) INPA conceptual diagram. (middle) Energy and spatial distribution of energetic neutrals before EIC excitation. (right) Distribution after EIC excitation. Energetic neutral distribution changed.

[1] W. Paenthong *et al.*, “Design and initial results of the imaging neutral particle analyzer in large helical device”, *Review of Scientific Instruments* **95**, 083547 (2024).
 [2] W. Paenthong *et al.*, “Observation of Helically-Trapped Energetic Particle Transport Induced by Energetic-Ion-Driven Resistive Interchange Mode using Imaging Neutral Particle Analyzer in Large Helical Device”, 51st European Physical Society Conference on Plasma Physics 2025, EPS25-0108.

(K. Ogawa)

Analyzing physics properties of plasma in newly designed device that controls hidden symmetry of magnetic field

Non-axisymmetric toroidal magnetic configurations that exhibit “hidden symmetry” in magnetic field strength have attracted particular attention, as they offer a steady-state operation while maintaining good particle confinement. To elucidate how magnetic configuration affects the degradation of plasma confinement due to collective phenomena such as instabilities, a comparative study between different magnetic configurations is demanded. We have designed a new experimental device that can control the hidden symmetry of a magnetic configuration, as shown in Fig. 1, applying an advanced coil optimization technique developed in the SFS Unit. We have conducted numerical analyses to predict the experimental capabilities of this device from various aspects, including magnetohydrodynamic (MHD) equilibrium, MHD stability, micro-instabilities and turbulence, particle orbits, and plasma heating [1]. One notable finding was the difference in the confinement of energetic particles between the two representative magnetic configurations. In the quasi-axisymmetric configuration, energetic ions with small velocity in the direction of the field line are easily lost due to the imperfection of axisymmetry. In the other configuration that exhibits a strong toroidal mirror, those energetic ions are found to be confined well. We also confirmed that MHD equilibria of different magnetic configurations can be achieved at a peak beta of approximately 4% without a significant break of magnetic surfaces. These findings enable us to plan plausible experimental scenarios, including academic research, such as observing phase-space dynamics during instabilities excited by energetic particles.

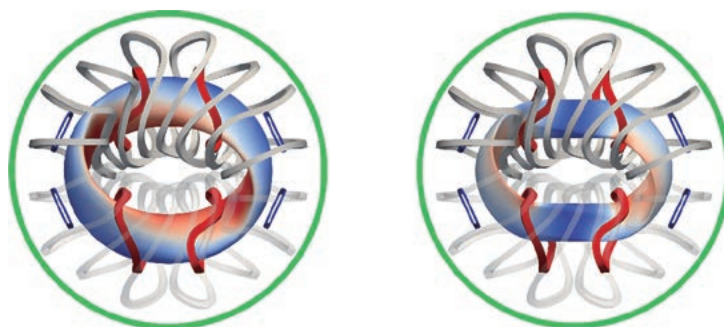


Fig. 1 The coil design and magnetic surfaces with different symmetry that can be generated by the same coils.

[1] H. Yamaguchi *et al.*, The 41st JSPF Annual Meeting, Nov. 17–20, 2024, Tokyo.

(H. Yamaguchi)

Phase Space Turbulence Unit

Highlight

Phase-space decomposed plasma distribution measurement and bifurcation in wave-particle interaction

A high-speed measurement of plasma distribution in phase-space was achieved using a data analysis method called phase-space tomography. Phase-space is expressed in terms of the coordinates of the position and velocity of plasma particles. Distortion of the plasma phase-space distribution can occur in high-temperature plasmas and is believed to have a significant impact on plasma performance. Spectroscopic measurements were applied to analyze the light emitted from plasma using three different types of devices, and a distortion of the plasma phase-space distribution was identified with high precision, using phase-space tomography. The distortion was found to form as a result of efficient plasma heating mediated by waves. Observation of plasma phase-space distribution is an important theme not only in fusion plasmas but also in plasma research on celestial bodies, the sun, and auroras, and is expected to have a ripple effect.

Fusion energy is being developed as a new source of clean electricity to help realize a carbon-neutral society. Plasma differs from regular gases in that it is extremely low in density—about one-millionth that of the atmosphere—so particle collisions are rare. As a result, the histogram of particle motion, called the velocity distribution function, can be distorted from the so-called Maxwell-Boltzmann distribution (equivalent to normal distribution). Such distortions can trigger unexpected plasma behavior, including sudden temperature changes and current generation, making it vital to understand these dynamics.

To analyze plasma motion, scientists commonly use spectroscopy to measure light emitted by plasma. However, because only a limited amount of light is available, spatial resolution has to be given up to measure quick time variations of the velocity distribution function. Yet, understanding how plasma evolves in both space and velocity (phase space) is key for controlling it and achieving efficient fusion power.

A high-speed measurement of plasma phase distribution with high precision was recently achieved by utilizing tomography technology used in the medical field. By combining a newly developed “high-speed luminescence intensity monitor” with existing spectrometers and synchronizing their operation, the plasma’s phase-space distribution was reconstructed. This enabled measurements at an unprecedented speed of 10,000 Hz—50 times faster than the previous 200 Hz standard.

Using this technique, energy exchanges between plasma and injected beam particles were observed in the LHD. Particles traveling at speeds close to wave velocities were accelerated, much like surfers riding ocean waves. These wave-particle interactions are crucial for heating plasma in fusion reactors. The study also revealed that waves propagating in opposite directions can occur simultaneously, enhancing particle acceleration and potentially improving heating efficiency [1] (Fig. 1).

This research demonstrates that coordinated diagnostics and data integration can achieve breakthroughs beyond the capabilities of individual instruments. The new method offers a powerful tool for future plasma control and fusion research. Furthermore, because collisionless plasmas also exist in astrophysical phenomena like the Sun and auroras, phase-space tomography may contribute to a wide range of scientific fields.

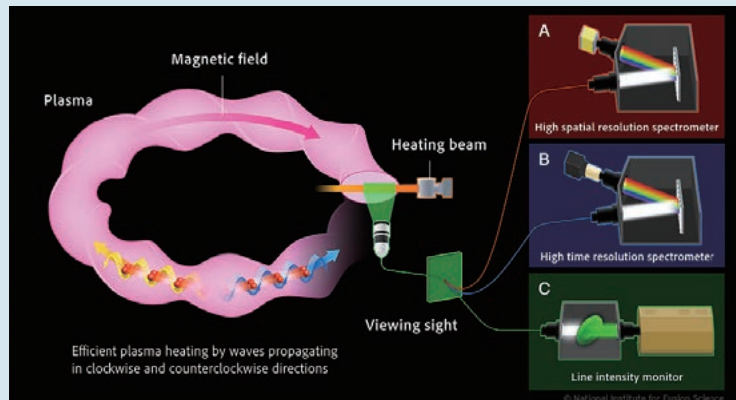


Fig. 1 Image of obtained physical picture by the phase-space tomography.

[1] Tatsuya Kobayashi, Mikirou Yoshinuma, Wenqing Hu, and Katsumi Ida, Detection of bifurcation in phase-space perturbative structures across transient wave – particle interaction in laboratory plasmas, The Proceedings of the National Academy of Sciences (PNAS) **121**, e2408112121 (2024).

(T. Kobayashi)

Development of Hyperspectral Camera for Auroral Imaging

The aurora is a natural luminous phenomenon caused by interactions between precipitating particles and the constituents of the upper atmosphere. The interaction between electromagnetic waves and particles that occur in the Earth's magnetosphere is thought to be an important mechanism for accelerating electrons, which causes the aurora to glow. This phenomenon of particles accelerating due to the interaction between electromagnetic waves and particles has also been observed in the Large Helical Device (LHD) and has attracted attention as a common energy transport process.

Based on the knowledge gained through the development of diagnostics to investigate such acceleration mechanisms, we developed a hyperspectral camera (HySCAI) for observing the aurora, to study auroral emission processes and colors in detail [1]. A hyperspectral camera can obtain a two-dimensional distribution of the spectrum, and is effective for observing the spectrum of auroras, which appear freely across the sky.

To actualize the hyperspectral camera, a galvanometer mirror scanner was used to scan the slit image on an all-sky image plane in a direction perpendicular to the slit. A high throughput lens spectrometer with an EMCCD detector was used to acquire the spectra image of the light coming from the slit. The spectrometer was equipped with two gratings, one 500 grooves/mm for a wide spectral coverage of 400–800 nm, and the other 1500 grooves/mm for a higher spectral resolution. By changing these grating constants and acquiring hyperspectral data with wide spectral coverage or higher wavelength resolution, new applications of hyperspectral data in aurora observation can be explored.

Initially, HySCAI had been designed to cover only half the sky for higher elevation angles. At the start of the season in 2024, it was redesigned and succeeded in acquiring spectral hyper data covering all the sky.

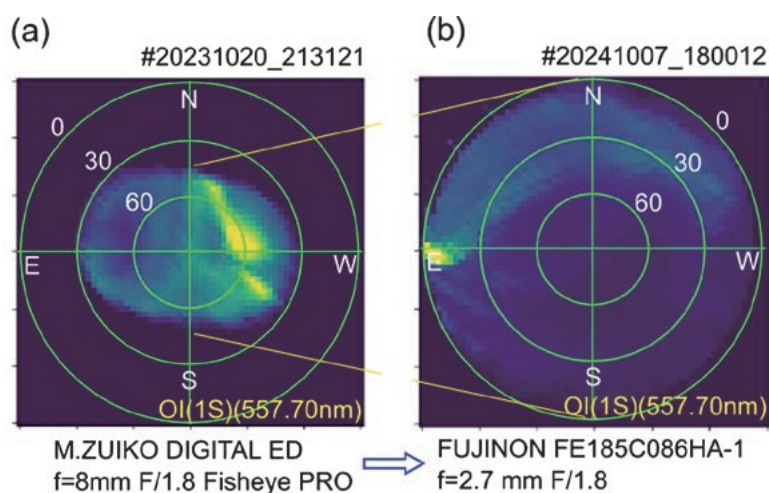


Fig. 1 Two-dimensional distribution images of OI(557.7nm) taken with HySCAI (a) before and (a) after expanding the field of view. This modification made it possible to obtain hyperspectral data covering all the sky.

[1] Yoshinuma, M., Ida, K. and Ebihara, Y. Development of hyperspectral camera for auroral imaging (HySCAI). *Earth Planets Space* **76**, 96 (2024). <https://doi.org/10.1186/s40623-024-02039-y>

Discovery of Spontaneous Inflow and Outflow States in High-Temperature Plasma Induced by Energetic Ion Anisotropy

In fusion research, the performance of magnetically confined plasma is determined by its density, temperature, and confinement time, all of which are strongly influenced by the heating conditions. Achieving a high-performance fusion reactor requires improving the confinement of particles and heat and maintaining high density and temperature in the core region, where fusion reactions occur.

In this study, we employed a neutral beam injection (NBI) system to heat the plasma and investigated how varying the ratio of tangential to perpendicular beam powers affected plasma behavior. We discovered that the inflow and outflow of high-temperature plasma are spontaneously regulated by a distinct state of energetic ions [1-4]. This novel finding may lead to the development of high-performance plasmas, reduction in reactor size, enhanced fusion power output, and improved control of plasma burning conditions.

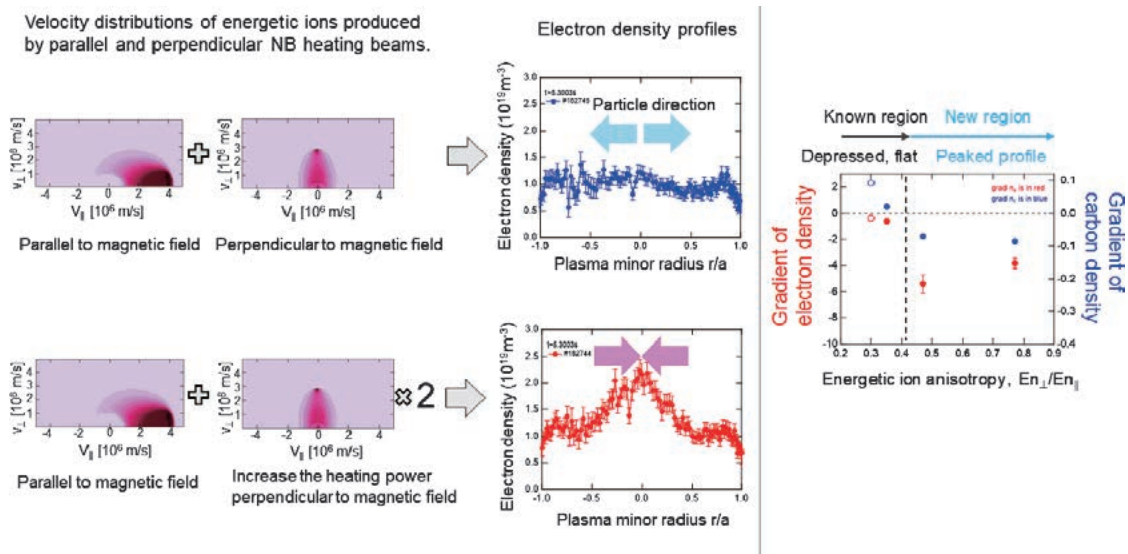


Fig. 1 (Left) Velocity distributions of heating beams injected parallel and perpendicular to the magnetic field. By varying the anisotropy of energetic ions, the electron density profile transitions between peaked and flattened shapes. The spatial profile is plotted as a function of the normalized plasma radius r/a , where $r/a = 0$ corresponds to the plasma center and $r/a = 1$ to the edge of the confinement region in the LHD. (Right) Electron and impurity density gradients as a function of the anisotropy parameter $En_{\perp}/En_{\parallel}$, where En_{\perp} and En_{\parallel} are evaluated from the total energy of particles in velocity space (v_{\perp} , v_{\parallel}). The results indicate that stronger anisotropy (higher $En_{\perp}/En_{\parallel}$) enhances central particle accumulation, while more isotropic distributions lead to flatter profiles and reduced confinement.

The Large Helical Device (LHD) is equipped with five NBI systems. NB#1 to NB#3 inject beams tangentially to the magnetic field, while NB#4 and NB#5 inject beams perpendicularly (Figure 1). Although the ratio of tangential to perpendicular power varied significantly, the ion temperature profile remained essentially unchanged. However, the middle panel of Figure 1 reveals that the electron density profile transitioned between peaked (red) and flat (blue) states, depending on the beam configuration.

By varying the power ratio of tangential and perpendicular beams, the velocity distribution of energetic ions shifts from isotropic to anisotropic. The right panel in Figure 1 shows how the electron density profile depends

on the energetic ion anisotropy, represented by the ratio of stored energy in the perpendicular and parallel components ($En_{\perp}/En_{\parallel}$), derived from the injected beam powers. When $En_{\perp}/En_{\parallel}$ was adjusted from 0.3 to 0.8, we found that profiles remained flat for $En_{\perp}/En_{\parallel} < 0.4$ and became centrally peaked for $En_{\perp}/En_{\parallel} > 0.4$. To further examine this effect, a carbon pellet was injected, and the resulting carbon ion density profiles were observed. The profile was hollow for $En_{\perp}/En_{\parallel} < 0.4$ but became peaked when $En_{\perp}/En_{\parallel} > 0.4$.

These results demonstrate that plasma transport and the balance of particle inflow and outflow can spontaneously change in the presence of anisotropic energetic ions. This has important implications for the control of the confinement region in fusion plasmas. To explore the underlying physics, simulation studies were carried out. First, we analyzed the radial electric field in the plasma core, which was found to be approximately -5 kV/m, consistent with heavy ion beam probe measurements. Although this field strength alone is unlikely to affect particle transport significantly, we further investigated the role of turbulence. The results suggest that turbulent transport plays a key role in determining whether the density profile is peaked or flat.

Our discovery reveals that the direction and magnitude of particle inflow and outflow within the confinement region can be effectively controlled by leveraging the anisotropic properties of energetic ions. This represents a significant advancement in the understanding of plasma transport physics and opens new pathways for optimizing confinement in future fusion reactors. In future work, we aim to elucidate the detailed physical mechanisms behind this phenomenon and apply our findings to enhance fusion plasma performance, downsize reactor designs, improve energy output, and enable robust control of burning plasmas.

- [1] M. Nishiura, “Core density profile control by energetic ion anisotropy in LHD”, 65th Annual Meeting of the APS Division of Plasma Physics, October 30–November 3, 2023 (invited).
- [2] M. Nishiura, “Particle transport control by auxiliary heating systems in LHD”, 24th International Stellarator Heliotron Workshop, 9–13 September 2024, Hiroshima, Japan (invited).
- [3] M. Nishiura *et al.*, “Core density profile control by energetic ion anisotropy in LHD” *Phys. Plasmas* **31**, 062505 (2024). <https://doi.org/10.1063/5.0201440>
- [4] Press Release, June 24, 2024, National Institute for Fusion Science and Kyushu University:
<https://www.nifs.ac.jp/news/collabo/240624.html>
<https://www.kyushu-u.ac.jp/ja/researches/view/1102/>
<https://www.eurekalert.org/news-releases/1048779>

(M. Nishiura)

Plasma Quantum Processes Unit

The goals of the Plasma Quantum Processes Unit are to advance interdisciplinary plasma research based on quantum processes and to promote international collaborations. Toward these goals, each member of the Unit is pursuing research with the following academic strategies.

Advancement

- Advancement of plasma measurement based on highly charged ion spectroscopy/quantum processes
- Inclusion of quantum physics in plasma kinetics and enhancement of the accuracy of kinetic transport calculations, including highly charged ions
- Fusion reactor edge plasma modeling, including atom-molecule processes and plasma-wall interactions

Interdisciplinary

- Collaboration with other fields using atomic and molecular data/promoting applications by developing databases
- Research on ultra-relativistic plasma dynamics, including quantum electrodynamics processes, and development of laboratory astrophysics using intense lasers
- Promoting collaboration with other Units and interdisciplinary research with physics fields other than fusion from the viewpoint of data-driven science and materials informatics for advanced measurements
- Interdisciplinary collaboration with particle physics fields through research on quark-gluon plasma, and obtaining hints for new measurements in fusion plasma experiments from detectors in high-energy accelerator experiments
- Applying cryogenic engineering technology developed in fusion research to high-energy density sciences

To ensure that the Unit’s research activities are carried out with the participation of the broader academic community, a Unit Research Strategy Council was organized, inviting 15 external members from various research fields.

The Unit regularly holds seminars with external collaborators to disseminate its research activities. Between April 2024 and March 2025, seven seminars were held on relevant topics, including atomic structure calculations of highly charged ions, highly charged ion spectroscopy, data-driven science, and lattice QCD simulations for quark-gluon plasma.

The Unit is developing numerical databases of atomic collisions and ion surface collisions for fusion and plasma applications through international collaborations. The databases are available on the internet (<https://dbshino.nifs.ac.jp/index-j.html>).

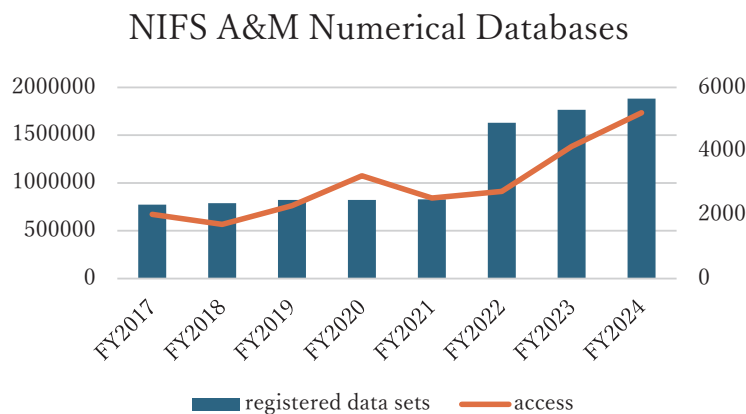


Fig. Annual changes in the number of registered data sets (left) and access (right) to the NIFS database. The number of data sets is as of the end of each fiscal year, and total access was counted in each fiscal year.

(I. Murakami)

Highlight

Development of Open Data Analysis Tool for Science and Engineering (ODAT-SE) in measurement informatics

A fundamental topic in fusion science and other scientific fields is measurement informatics, the methodology of data analysis in experimental measurements. As an interdisciplinary research activity, we have released an open-source software Open Data Analysis Tool for Science and Engineering (ODAT-SE), formerly known as 2DMAT, for the data analysis of many advanced experimental measurements (<https://github.com/issp-center-dev/ODAT-SE>). ODAT-SE can be applied to a new experimental measurement method by adding a model for the experimental measurement. Currently, ODAT-SE offers five analysis methods: (i) grid search, (ii) Nelder-Mead optimization, (iii) Bayesian optimization, (iv) the replica exchange Monte Carlo method, and (v) the population-annealing Monte Carlo (PAMC) method. In particular, the PAMC method uses massively parallel Bayesian inference and is suitable for supercomputers like Fugaku. In general, the Bayesian inference gives posterior probability distribution $P(X|Y)$, as a histogram of Fig. 1(a), where $X \equiv (X_1, X_2, \dots, X_n)$ is the target quantity (vector), the quantity that we would like to know, and $Y \equiv (Y_1, Y_2, \dots, Y_m)$ is the experimentally observed quantity (vector). Since the PAMC method is a global search algorithm, one can find global and local solutions in the data space of X . In a recent paper, the PAMC method was used to determine the surface structure of the 3×3 -Si phase on the Al (111) surface using total reflection high-energy positron diffraction (<https://www2.kek.jp/imss/spf/eng/>, Fig. 1(b)) and core-level photoemission spectroscopy [1]. The analysis finds the global solution as a flat surface structure shown in Fig. 1(c) and local solutions, which indicates the crucial importance of the global search algorithm. As a future project, ODAT-SE will be developed further and used both in plasma and material science, for example, through our project launched recently in the Moonshot R&D Program (https://www.jst.go.jp/moonshot/en/program/goal10/A3_hoshi.html).

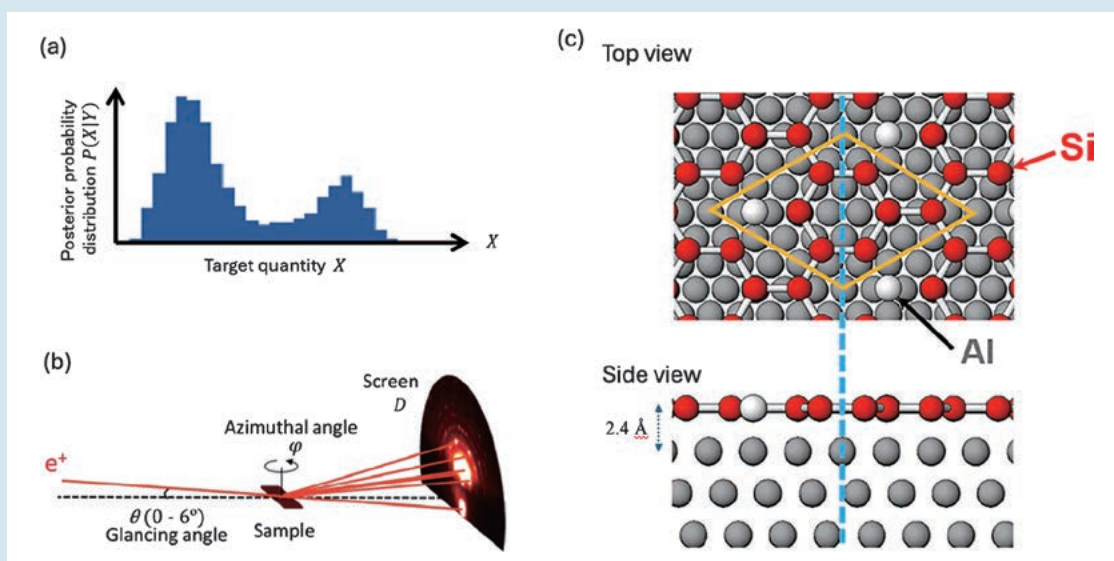


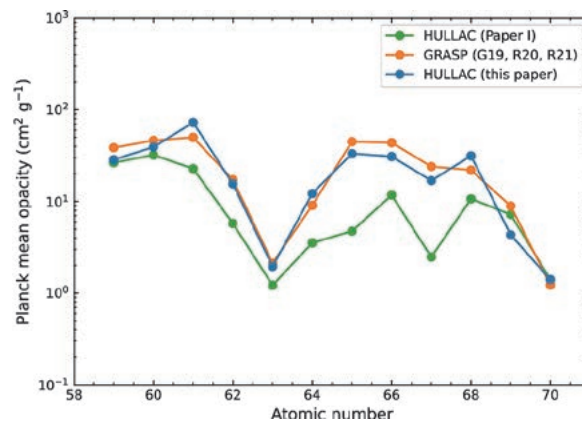
Fig. 1 (a) Schematic diagram of posterior probability distribution $P(X|Y)$ (b) Schematic diagram of total reflection high-energy positron diffraction experiment (c) Top view (upper panel) and side view (lower panel) of surface structure of the 3×3 -Si phase on Al (111) surface [1].

[1] Y. Sato *et al.*, Phys. Rev. Materials **9**, 014002 (2025).

Systematic opacity calculations for kilonovae – II. Improved atomic data for singly ionized lanthanides [1]

Lanthanides play most important roles in the opacities for kilonovae, ultraviolet-optical-infrared emissions from neutron star mergers. Although several efforts have been made to construct atomic data, the accuracy of the opacity has not been fully assessed and understood. Due to the complexity of the atomic structures of the lanthanides, theoretical atomic calculations covering many elements and ionization stages often involve simplifications in the calculations, such as a parametrized effective potential. In this paper, we aim to obtain a deeper understanding of the lanthanide opacities in kilonova ejecta, and at finding a strategy to provide accurate atomic data with the parametric potential method using the Hullac code, which has been utilized for spectral analysis of impurity ions in LHD plasmas.

Firstly, we identified transition arrays which are relevant to structures in the opacities, for which derivation of accurate energy level distribution is important to obtain reliable opacities. Then, we optimized the parametric potential to minimize configuration averaged energies of the transition arrays. The opacities evaluated with our new results were higher by a factor of up to 3–10 compared with our previous work [2] (Paper I, see Figure), which agreed with opacities obtained by more time-consuming benchmark calculations using the Grasp2K code [3-5].



Planck mean opacities of singly ionized lanthanides for density of 10^{-13} g/cm³ and temperature of 5,000 K at 1 day after the merger [1].

- [1] D. Kato, M. Tanaka, G. Gaigalas, L. Kitovienė, P. Rynkun, Monthly Notices of the Royal Astronomical Society **535**(3), 2670–2686 (2024).
- [2] M. Tanaka, D. Kato, G. Gaigalas, K. Kawaguchi, Monthly Notices of the Royal Astronomical Society **496**(2), 1369–1392 (2020).
- [3] G. Gaigalas, D. Kato, P. Rynkun, L. Radžiūtė, M. Tanaka, The Astrophysical Journal Supplement Series **240**, 29 (2019).
- [4] L. Radžiūtė, G. Gaigalas, D. Kato, P. Rynkun, M. Tanaka, The Astrophysical Journal Supplement Series **248**, 17 (2020).
- [5] L. Radžiūtė, G. Gaigalas, D. Kato, P. Rynkun, M. Tanaka, The Astrophysical Journal Supplement Series **257**, 29 (2021).

(D. Kato)

Transport in Plasma Multi-phase Matter System Unit

The term “multi-phase” refers to the three states of matter: solid, liquid, and gas. In the region where the fourth state of matter, plasma, meets the other three, many interesting phenomena occur. In a fusion reactor, relatively cold plasma surrounding the hot core plasma comes into contact with the reactor wall made from solid or sometimes liquid materials.

The research objective of this unit is to investigate the behavior of plasma, gases and wall materials in the region where they interact with each other, through experiments and computer simulations. To be more specific, our research goal is to understand the particle and energy transport of boundary plasma and to investigate the effects of plasma interactions on materials that alter these properties.

Knowledge and techniques gained in our study are applied not only to plasma and fusion research but other research fields, e.g., materials science, bioengineering and various industrial technologies. Many domestic and international collaborations with universities, laboratories and private sectors are being conducted.

The following are the results obtained in this Unit.

1. Spatial Distribution of Hydrogen Molecules in the Divertor Region of JA-DEMO

Seiki Saito, Hiroaki Nakamura *et al.* performed a molecular dynamics simulation to estimate the rovibrational states of recycled hydrogen molecules in the divertor region of the JA-DEMO reactor under detached plasma conditions. In this region, it is well known that the rate coefficient of molecular-assisted recombination (MAR) varies by several orders of magnitude, depending on the rovibrational states of the hydrogen molecules.

They revealed in the simulations that molecules in higher rovibrational states (more than 15) are released even with low incident energy, which is expected to be the dominant condition under detached plasma conditions. Molecules generated in this way can strongly affect the formation of the detached plasma via a molecular assisted-process such as MAR.

These findings mentioned above were published in Nucl. Fusion 64 (2024) 126067.

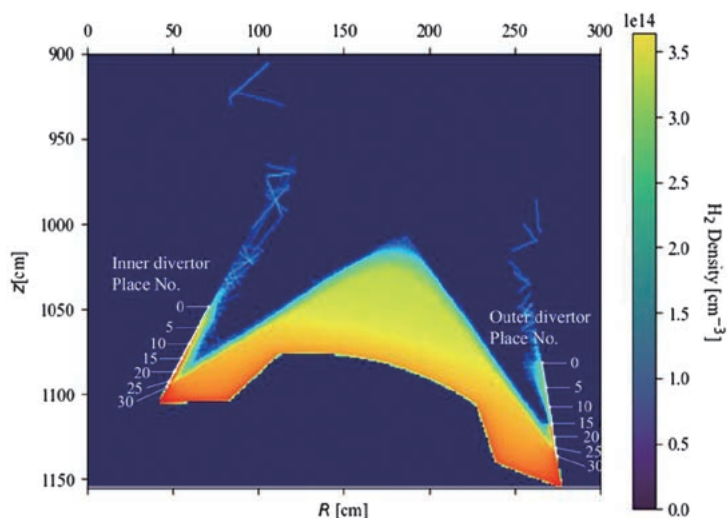


Fig. 1 Spatial distribution of density of hydrogen molecules calculated by the neutral transport (NT) simulation with the emission distribution at the wall calculated by the MD simulation.

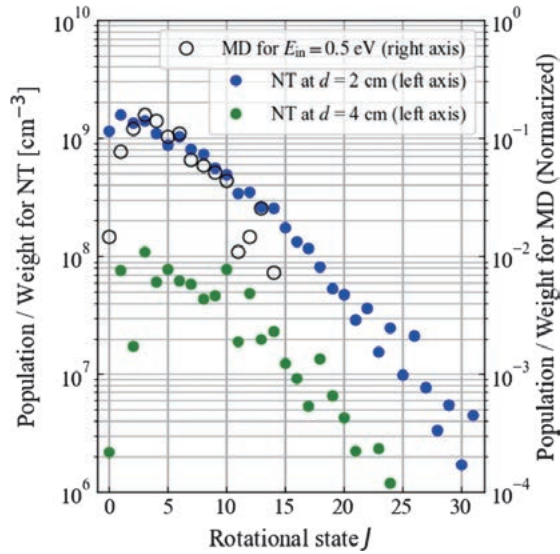


Fig. 2 Distributions of rotational states J of hydrogen molecules.

2. Propagation characteristics of the millimeter-wave vortex in magnetized plasma

Chenxu Wang, Hideki Kawaguchi, Hiroaki Nakamura and Shin Kubo investigated the propagation characteristics of a millimeter-wave vortex of a hybrid mode of a cylindrical corrugated waveguide in the magnetized plasma by using three-dimensional numerical simulations with the finite-difference time-domain (FDTD)

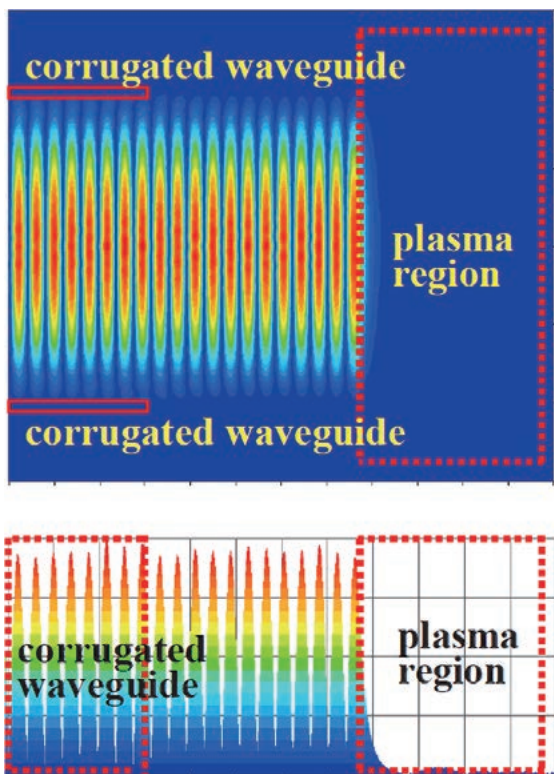


Fig. 3 Electric field intensity in the y - z plane with $l = 0$ (plane wave).

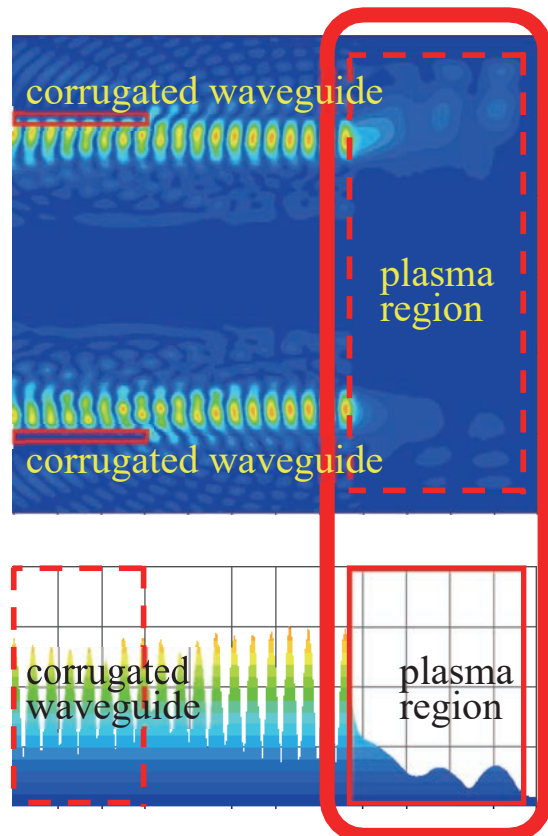


Fig. 4 Electric field intensity in the y - z plane with $l = 20$ (millimeter-wave vortex of a hybrid mode).

method. They revealed that the millimeter-wave vortex of the hybrid mode can propagate in magnetized plasma even under conditions where a normal plane wave is cut off. Moreover, the propagation power in the plasma is highly dependent on the topological charge.

These findings mentioned above were published in Japanese Journal of Applied Physics 63, 09SP08 (2024).

3. Real-Time Boronization Using an Impurity Powder Dropper in LHD

Suguru Masuzaki, Mamoru Shoji *et al.*, performed a real-time boronization using an impurity powder dropper (IPD) during discharges. The result was compared with that of a conventional glow discharge boronization with diborane gas, performed before each experimental campaign.

In both methods, oxygen and iron impurities were effectively reduced. In glow discharge boronization, the reduction in oxygen levels persisted until the end of the experimental campaign. On the other hand, reduction in iron levels only lasted a few days. In the case of the real-time boronization with the IPD during long pulse discharges, suppression of both the oxygen and iron was observed. The effect on the iron quickly diminished within several seconds after the injection ended, whereas the effect on the oxygen lasted more than 100 s.

These findings mentioned above were published in Nuclear Materials and Energy 42 (2025) 101843.

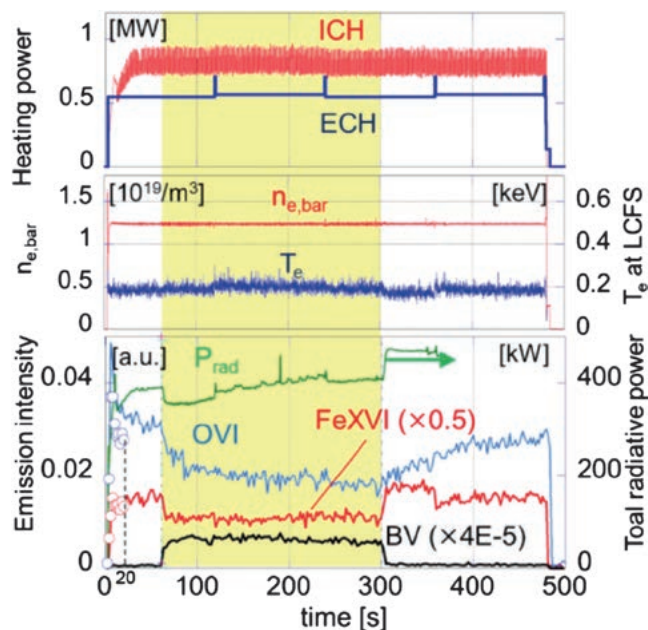


Fig. 5 Time evolutions of heating power, line average density and electron temperature at LCFS, radiative power, line emission intensities of iron, oxygen, and boron during discharge #176017. B dropped from 60.8 s to 300.8 s. Blue and red open circles represent the OVI and FeXVI intensities, respectively, for discharge #176018, where the discharge conditions were identical to those of discharge #176017 for the first 20 s.

Sensing and Intellectualizing Technology Unit (S&I)

This chapter reports on the two major results achieved by the S&I Unit in FY2024. The S&I unit consists of plasma scientists from various fields. Collaborations and discussions within this group produce synergistic effects for new findings and developments. One result concerns the MHD physics of high-temperature magnetic confinement. The other is the development of new nano-manufacturing technology.

Both results are based on precise plasma diagnostics and laser engineering developed within this unit.

Parity transition of radial structure of MHD instability in magnetically confined torus plasmas

The parity transition of radial displacement profiles associated with MHD instabilities is closely related to the formation and stabilization of magnetic islands in magnetically confined plasmas. Odd parity typically indicates the presence of a distinct magnetic island, while even parity suggests its absence. This study investigates the influence of externally applied resonant magnetic perturbations (RMPs) on the characteristics of parity transitions, with the aim of achieving active control of magnetic islands via parity modulation.

Odd-to-even parity transitions have never been observed in other devices. In this study, both even-to-odd and odd-to-even transitions were identified within a single discharge in the Large Helical Device (LHD). In discharges where the $m/n = 1/1$ resistive interchange mode (RIC), an even-parity MHD instability, remains unstable, an increase in electron density leads to the emergence of an $m/n = 1/1$ instability accompanied by a magnetic island—referred to as the “Edge” MHD instability—which then triggers a parity transition from even to odd. When the Edge instability subsequently stabilizes while RIC remains dominant, a transition from odd to even parity occurs. These observations indicate that the competition between the RIC and Edge instabilities governs the occurrence of parity transitions. Here, m and n represent the poloidal and toroidal mode numbers, respectively.

Figure 1 shows the time evolution of the magnetic island width (red symbols) in a large external RMP discharge. The island width was evaluated based on the peak-to-peak distance of the odd-parity structure measured by high-spatial-resolution CO₂ interferometry. Zero island width indicates even parity, while a finite width corresponds to odd parity. Figure 2 shows the dependence of odd-to-even parity transition frequency on the strength of external RMP. Although odd-to-even parity transitions can occur even with relatively small RMPs, their frequency increases sharply once the RMP amplitude exceeds a certain threshold. One possible explanation is that a stronger external RMP shortens the island formation time,

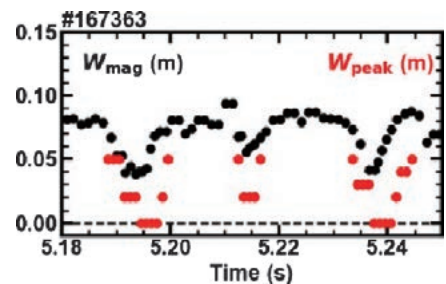


Fig. 1 Time evolution of magnetic island width in a discharge with a large RMP, showing frequent parity transitions. (Reproduced from Takemura *et al.*, *Sci. Rep.* **15**, 14890 (2025))

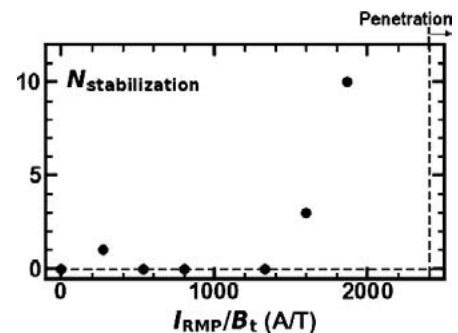


Fig. 2 The number of occurrences of the odd-to-even parity transition in discharges with the same experimental conditions except for external RMP amplitude. (Reproduced from Takemura *et al.*, *Sci. Rep.* **15**, 14890 (2025))

thereby increasing the transition frequency.

In summary, our results show that the frequency of parity transitions—including the newly observed odd-to-even type—can be actively controlled by external RMPs. This provides new insights into magnetic island dynamics and suggests strategies for active control of magnetic islands in future fusion reactors.

[1] Y. Takemura *et al.*, *Scientific Reports* **15**, 14890 (2025).

(Y. Takemura)

Plasma Nanofabrication on Various Semiconductors by the Codeposition Etching Technique [2]

This study explores a lithography-free nanofabrication method known as Codeposition Etching (CoDE), applied for the first time to various compound semiconductors using argon plasma and molybdenum (Mo) impurities. Unlike conventional nanostructure fabrication that relies on complex techniques like photolithography and reactive ion etching, CoDE offers a simple, one-step alternative to create nano/microstructures based on the interaction between impurity deposition and plasma etching.

In the CoDE process, Mo atoms are co-deposited onto semiconductor surfaces during Ar plasma irradiation. These atoms act as nanomasks due to their lower sputtering yield compared to the substrate, enabling the selective formation of nanostructures through preferential sputtering. Experiments were performed on six different semiconductors: Si, SiC, Ge, GaAs, ZnSe, and GaN. Structures were successfully formed on Ge, GaAs, ZnSe, and GaN, but not on Si and SiC, consistent with their lower sputtering yields relative to Mo.

The study investigates the effects of impurity flux and deposition time. Increasing the Mo deposition rate (via a biased Mo wire) resulted in higher density and smaller-size structures, although their height was reduced due to decreased selectivity in sputtering. Notably, the structures evolved from conical shapes to more complex hillock or dislocation forms at higher impurity concentrations, suggesting a shift in the nucleation mechanism. Time-dependent experiments revealed a threshold behavior in structure formation, indicating a critical impurity concentration required to trigger uniform nucleation—akin to crystal growth in supersaturated solutions.

The authors propose a four-step mechanism: (1) impurity deposition, (2) surface diffusion, (3) nucleation via either defect trapping or supersaturation, and (4) preferential sputtering. This model highlights the tunability of structure size and density through control of impurity flux and substrate properties.

In conclusion, CoDE proves to be a promising approach for scalable, cost-effective nanofabrication on a broad range of semiconductor materials. It holds potential for applications in photovoltaics, optoelectronics, and random lasers, where surface morphology rather than precise patterning is critical. Future research will address the roles of temperature, impurity species, and further optimization for practical applications.

[2] Q. Shi, S. Kajita, N. Ohno, H. Tanaka, R. Yasuhara, H. Fujiwara, and H. Uehara, Lithography-Free Nanofabrication on Various Semiconductors by the Codeposition Etching Technique. *Langmuir* **40**(24), 12437–12442 (2024).

(H. Uehara)

Plasma Apparatus Unit

The plasma apparatus (PA) unit, a core component of plasma science and technology, started in fiscal 2023. The importance of disruptive innovation as a game-changer in fusion research has been pointed out. To this end, the PA unit will aspire to create innovative plasma technologies by deepening scientific knowledge of the complex collective phenomena of plasma. By developing novel applications of plasma as working hypotheses, the PA unit will promote collaboration in fusion with other fields and shed light on the unexplored emergent nature of collective phenomena. Innovations in plasma science and technology will open a new horizon for various natural science research, other disciplines and technologies.

Toward the above end, the following research topics were pursued: neutral beam injection, anti-matter and dipole plasma, and muon science.

(H. Nakano)

Neutral Beam Injector

One of the issues in ITER Neutral-Beam (NB) development is reducing the beam divergence of the Radio Frequency (RF) negative hydrogen ion source. Especially in the Diagnostic NB (DNB) with 100 keV in beam energy, the beam divergence has not met the ITER requirement with which the NIFS-NB Filament-driven Arc (FA) ion source is satisfied. The beam divergences of FA and RF ion sources have been compared using the FA/RF hybrid Research and development Negative Ion Source (NIFS-RNIS), upgraded from the original NIFS-RNIS, a FA negative ion source, through collaboration with NIFS, the ITER organization, and the Max Planck Institute for Plasma Physics. This year, an increase in negative hydrogen ion density by cesium seeding was observed for the first time. In a well-cesiated condition, the original FA NIFS-RNIS and the FA/RF hybrid NIFS-RNIS with RF-mode, with around 50 keV in beam energy, formed a beam with a similar beam divergence angle of 9 mrad under the assumption of a beam size as a point at the grounded grid electrode (GG) of the ion source accelerator. The beam divergence of 9 mrad satisfies the ITER requirement of 7 mrad when the beam diameter at the GG is 5 mm.

Low-pressure operation in the ion source discharge chamber enhances efficiency by reducing stripping losses in the beam extraction and acceleration regions. In exploring the lowest operating pressures for hydrogen and deuterium in the current setup, the FA/RF hybrid NIFS-RNIS, it was found that the minimum operating pressure for deuterium was lower than that for hydrogen in RF-mode. Another isotope effect was also observed in the investigation using the original FA NIFS-RNIS, where the line-averaged negative ion density of the deuterium was higher than that of hydrogen in RF mode.

Toward the realization of a cesium-free negative-ion source, C12A7 electride was tested as the plasma-facing grid of the ion source accelerator using an induced-coupled plasma ion source with 1 kW discharge power installed in the Equipment with Versatility for Ion Source Study (EVISS). Comparing the reference material for aluminum alloy, a 70 % larger beam current was observed.

(H. Nakano)

Anti-Matter and Dipole Plasma

In the development of an electron–positron plasma experiment, a positron trap employing a 5 T superconducting magnet was successfully operated, demonstrating stable confinement of pure electron plasmas. The trap has been integrated with a low-energy positron beamline at AIST, and preliminary positron injection tests have been conducted. In parallel, a levitated high-temperature superconducting dipole device has been designed and fabricated, including cryogenic and vacuum components. Numerical orbit analyses revealed that the radial mixing between electrons and positrons is intrinsically difficult but can be enhanced by introducing chaotic orbits and rotating electric fields, suggesting a viable pathway toward creating confined pair plasmas. In a laboratory study of wave particle interactions and transport in a dipole field, experiments with the RT-1 device at the University of Tokyo demonstrated radial particle transport driven by low-frequency electrostatic fluctuations. Synchronous measurements of magnetic fluctuations and energetic electron losses confirmed inward transport correlated with chorus emissions. The occurrence frequency of chorus emissions was found to depend on the magnetic field curvature, providing new insight into the link between magnetic geometry and self-organized plasma dynamics. These results indicate significant progress toward realizing laboratory pair plasmas and deepening the understanding of wave-driven transport common to both laboratory and space plasmas.

(H. Saito, Univ. Tokyo)

Muon Science

We have advanced muon science using superconducting transition-edge sensor (TES) microcalorimeters, achieving an unprecedented relative energy resolution of $\Delta E / E \sim 10^{-3}$. This technique enables precision X-ray spectroscopy of muonic atoms, offering a new approach to studying highly charged ions and providing a platform to explore quantum dynamics involving negatively charged particles such as muons and electrons bound to a single nucleus.

In FY2024, we achieved the first experimental observation of multicharged muonic ions, a novel atomic system where a negative muon replaces inner-shell electrons. Using high-resolution TES spectroscopy of low-pressure argon gas, we resolved X-ray peaks corresponding to one-, two-, and three-electron μAr states. These results confirm theoretically predicted structures and open the way to femtosecond-scale studies of muon–electron coupled dynamics.

We also conducted muonic X-ray experiments with newly developed high-energy TES detectors (up to 100 keV) to explore strong-field QED phenomena. In parallel, low-energy TES detectors (< 10 keV) are being applied to precision measurements that aim to elucidate the microscopic mechanisms of muon-catalyzed fusion (μCF).

This research, currently under consideration for inclusion in the JST Moonshot Goal 10 program, is expected to deepen fundamental understanding and contribute to the realization of high-efficiency μCF .

(S. Okada, Chubu Univ.)

Complex Global Simulation Unit

To understand the behavior of a multi-hierarchy system, individual simulations of each level are not sufficient. Global simulations that account for inter-hierarchy interactions are essential in nuclear fusion research and in many academic fields. They are challenging due to the vast differences in time and spatial scales. This unit develops methods that couple different hierarchies and physical models to overcome this difficulty. The unit focuses on (1) global simulations of magnetic confinement fusion plasmas—covering both core and edge—via kinetic-MHD hybrid methods, and (2) broadly applicable approaches to overcome computational limits and better reproduce real-world behavior. Notable progress was made in 2024–2025, as described below.

(H. Miura)

Strong impact of energetic ions on edge-localized modes in tokamak plasmas

The effects of energetic ions on the edge localized mode (ELM), a heat and particle ejection phenomenon in fusion plasmas was investigated using a kinetic-magnetohydrodynamic hybrid simulation code, MEGA [1], by an international collaboration involving researchers from the University of Seville, Spain, and the Complex Global Simulation Unit of the National Institute for Fusion Science.

The simulation reproduced an abrupt and large crash that characterizes ELMs, and revealed that energetic ions have a significant effect on the amplitude and frequency spectrum of ELMs [2]. A resonant interaction between the energetic ions at the plasma edge and the electromagnetic perturbations from the ELM leads to an energy and momentum exchange. This study advances the understanding of the physics underlying ELM crashes in the presence of energetic ions and highlights the importance of these ions in the optimization of ELM control techniques.

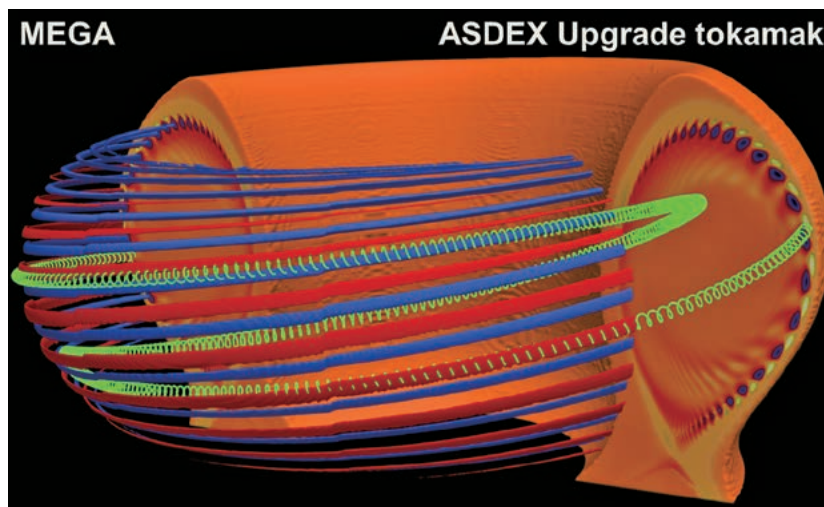


Fig. 1 3D visualization of an ELM in the ASDEX Upgrade tokamak, as simulated with the MEGA code. The tokamak volume is colored according to the ELM structure. The ELM interacts with the energetic ions whose orbit is shown in green. Figure adapted from J. Dominguez-Palacios *et al.*, Nat. Phys. (2025), under a Creative Commons license CC BY 4.0, <http://creativecommons.org/licenses/by/4.0/>.

[1] Y. Todo and T. Sato, *Physics of Plasmas* **5**, 1321 (1998).

[2] J. Dominguez-Palacios *et al.*, *Nature Physics* (2025). <https://doi.org/10.1038/s41567-024-02715-6>

(Y. Todo)

The nonlinear excitation of instability via resonance overlap in ASDEX-Upgrade tokamak

The Alfvén instability can nonlinearly excite the energetic-particle-driven geodesic acoustic mode (EGAM) on the ASDEX-Upgrade tokamak, as demonstrated experimentally. The mechanism of the EGAM excitation and its nonlinear evolution are not yet fully understood. In the present work, a first-principles simulation using the MEGA code investigated the mode properties in both the linear growth and nonlinear saturated phases, utilizing realistic parameters. The simulation successfully reproduced the experimental observations, including the excitation and coexistence of the Alfvén instability and EGAM [3]. The simulated mode properties are consistent with experimental results, achieving excellent validation. Conclusive evidence from the simulation identified resonance overlap as the excitation mechanism for the EGAM. In the linear growth phase, energetic particles satisfying different resonance conditions excited the Alfvén instability, leading to their redistribution in phase space. Subsequently, in the nonlinear saturated phase, these redistributed energetic particles moved into the EGAM resonance region, causing an overlap and thereby exciting the EGAM. Analysis of the total energetic particle distribution f_{total} confirmed the existence of regions with positive $\partial f/\partial E$ along conserved quantities, which are conducive to EGAM excitation. The above process is illustrated in Fig. 2. This work clarifies the mechanism of EGAM excitation by Alfvén instability, providing a robust explanation for the experimental observations.

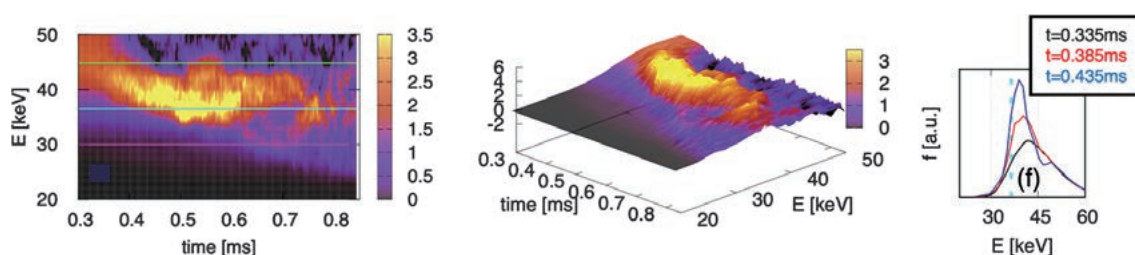


Fig. 2 (Left) The time evolution of f_{total} . The blue and cyan lines represent the Alfvén instability and EGAM resonance lines, respectively. (Middle) A 3-D bird's-eye view of the left subfigure. (Right) The f_{total} at different times, with the cyan dotted line indicating the EGAM resonance line.

[3] H. Wang, Ph. Lauber, Y. Todo *et al.*, *Scientific Reports* **15**, 1130 (2025).

(H. Wang)

The time evolution of information entropy and mutual information during the Landau damping process is elucidated

This study explores information entropy dynamics during Landau damping in a 1D Vlasov–Poisson system. Starting from a Maxwellian distribution with a cosine density perturbation, it derives linear and quasilinear solutions to describe early and late-time behavior, validated by contour dynamics simulations. Entropies of position and velocity distributions, and their mutual information, reveal statistical correlations beyond macroscopic descriptions. In weakly collisional regimes, mutual information vanishes while total entropy increases, consistent with the H-theorem. This work was published as K. Maekaku, H. Sugama, and T.-H. Watanabe, “Time evolutions of information entropies in a one-dimensional Vlasov–Poisson system”, *Phys. Plasmas* **31**, 102101 (2024) and was selected as a Featured Article.

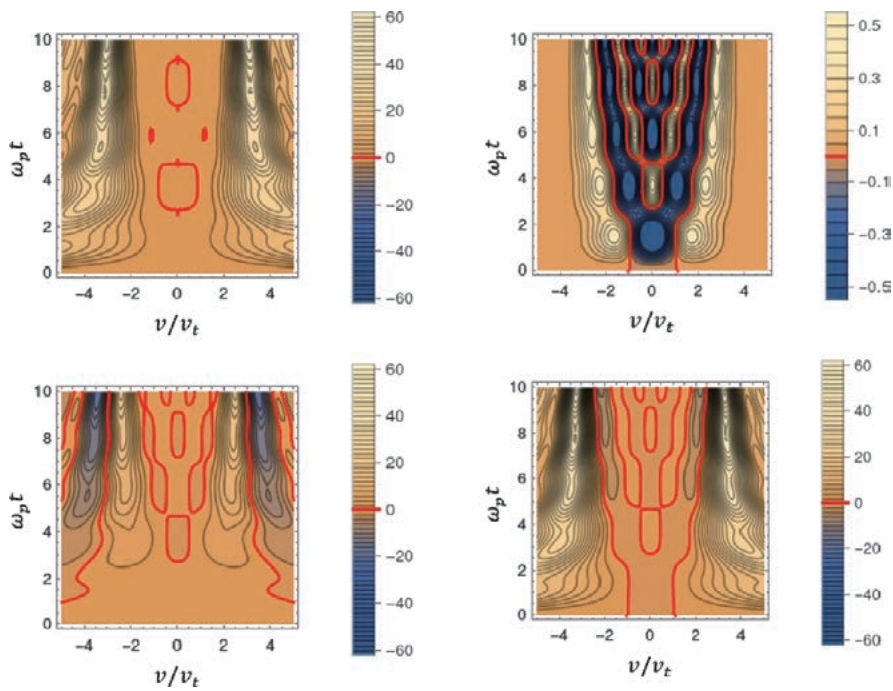


Fig. 3 Contours of the change in kinetic energy (top-left), self-entropy (bottom-left), deviation of the velocity distribution function from Maxwellian equilibrium $f_2(v, t)/(\alpha^2 n_0 v_i^{-3})$ (top-right), and $f_2(v, t)/(\alpha^2 f_{0M}(v))$ (bottom-right) on the (v, t) plane for $k\lambda_D = 1/2$. [Reproduced from K. Maekaku, H. Sugama, and T.-H. Watanabe, *Phys. Plasmas* **31**, 102101 (2024); licensed under CC BY.]

(H. Sugama)

Ultrahigh-flux Concentering Materials Unit (ULCoMat)

Highlight

Prediction, synthesis, and properties of accident-tolerant hybrid ceramics for fusion breeding blanket

In a deuterium–tritium fusion reactor, the breeding blanket surrounding the plasma contains Li compounds as tritium breeders in either solid or liquid form to convert the kinetic energy of the neutrons into heat and produce tritium fuel. In water-cooled ceramic breeding blankets for fusion reactors, hydrogen gas generation by steam oxidation of metallic Be compounds (i.e. neutron multipliers) in a loss-of-coolant accident (LOCA) raises major safety concerns. Li–Be hybrid ceramics have the potential to reduce hydrogen generation significantly. However, stable compositions and structures for quaternary compositions have not been comprehensively understood. In this work, as a collaboration study with the National Institutes for Quantum Science and Technology, we employed a machine-learning based prediction model CSPML (crystal structure prediction with machine learning-based element substitution) and experimentally synthesized chemically stable two-phase Li–Be–X–O hybrid ceramics [1]. The steam exposure tests demonstrated a negligibly small H_2 generation from the two-phase powder of Li_2BeSiO_4 with 5 at.% BeO below 1473 K. The stability is explained by the intrinsic ionic/covalent bonding characteristics and little capacity for further oxidation by steam. Particle transport calculations using the PHITS code with a simplified one-dimensional model showed that the Li_2BeSiO_4 –BeO mixture had comparable or slightly higher breeding performance without the use of metallic Be-based neutron multipliers. The hybrid ceramics represent the first example of a multi-functional oxide that can breed sufficient tritium fuel with no metallic neutron multiplier, enabling a novel design of ceramic breeding blankets with enhanced safety margins during in-box LOCA conditions.

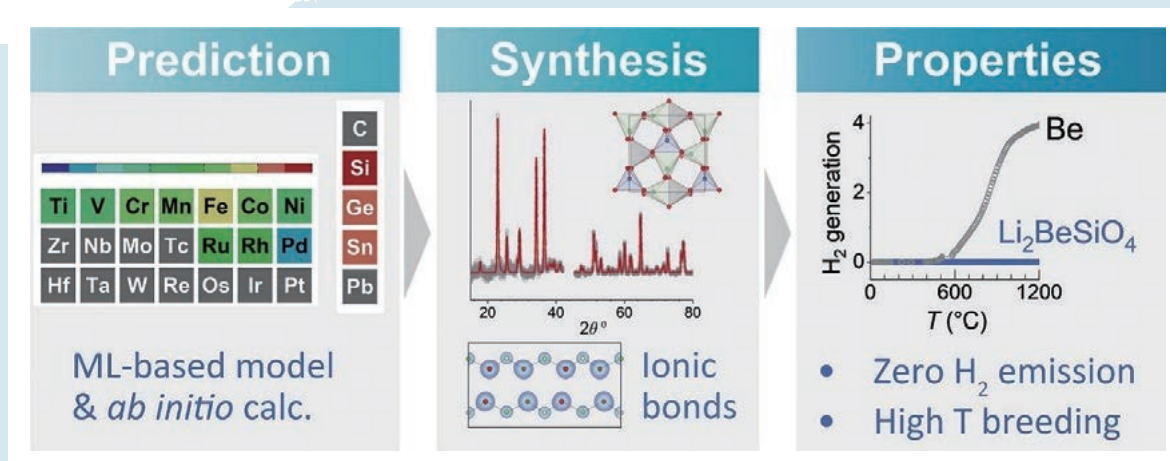


Fig. 1 Machine learning-based prediction, synthesis, crystal structure, high temperature chemical stability, and breeding performances of Li–Be hybrid ceramics.

(K. Mukai)

Small specimen test technique for fusion reactor materials

A small specimen test technique is essential to develop fusion reactor materials using a limited irradiation volume in a high-flux neutron field. An international collaboration activity “Towards the Standardization of Small Specimen Test Techniques for Fusion Applications” has been initiated under the framework of the International Atomic Energy Agency (IAEA) Coordinated Research Project (CRP). The project includes tensile, creep, low cycle fatigue, fracture toughness, and fracture crack growth rate testing. NIFS is taking part in the tensile and creep testing [2]. F82H IEA heat, an international reference RAFM steel, was evaluated at 550 and 650°C, using flat-plate specimens with gauge thickness ranging from 0.14 to 1.2 mm, while the gauge length and width were 5 and 1.2 mm, respectively. Tensile yield stress, ultimate tensile strength and uniform elongation were independent of the gauge thickness, and agreed with standard size specimen data. On the other hand, total elongation decreased with diminishing thickness. This behavior is attributed to the transition from symmetric diffuse necking to localized necking under plane stress conditions for the thinner specimens. Creep rupture time decreased with lessening gauge thickness. This is generally explained by enhanced creep deformation due to the annihilation of mobile dislocations around the surface.

(T. Nagasaka)

Influences of minor Ti addition on microstructure and tensile properties of high-purity V-10Cr alloys

V-4Cr-4Ti alloy is regarded as a promising candidate structure material for blanket applications in fusion reactors. To reduce the recycling period of vanadium alloy after use, high-purity vanadium alloys were developed. They contained much lower levels of high radioactive elements that could create long-lived isotopes under fusion neutron irradiation, such as cobalt, niobium, molybdenum, nickel, etc., and interstitial impurities (i.e., carbon, nitrogen, oxygen). Moreover, it suggested that further reducing the Ti concentration would shorten the cooling time of V-4Cr-4Ti alloy. However, the reduction of Ti decreased the strength, while increasing Cr concentration was expected to enhance it. Hence, a lower level of Ti (0.1 – 2 wt%) was added in vanadium alloys with a high-Cr level, and its effect on microstructure and tensile properties was investigated [3]. Results showed that precipitation was dependent on Ti concentration. Adding 0.5 wt% Ti was necessary to absorb those interstitial impurities forming Ti-rich precipitates, while a higher Ti content of 2 wt% prevented grain growth during thermal annealing. Furthermore, tensile strength increased with rising Ti concentration at both room temperature and 973 K, and elongation was not obviously changed. A minor Ti addition had a more evident effect on tensile strength at 973 K than that at room temperature. Additionally, further investigations on the microstructure evolution and irradiation hardening behaviors of those alloys after ion irradiation are in progress.

(J.J. Shen)

Application of a single crystal diamond detector for fast neutron measurements under high dose and mixed radiation fields

The developments of advanced scientific/engineering systems, including fusion reactors, usually require neutron measurements under a mixed and high-dose radiation field. In this study, we have developed a method to evaluate the fast neutron energy spectrum using a single-crystal chemical vapor deposition (CVD) diamond detector (SCDD), which can work under a high radiation dose field [4]. Also, a combination of pulse shape discrimination (PSD) based on the shape and width of a pulse with an unfolding technique for the measured spectrum could reject pulses by gamma-ray, and deduce the neutron energy spectrum.

For a demonstration of the present method, monoenergetic 14.1 MeV or 5.5 MeV neutron irradiation were carried out. The PSD was applied to a successful extraction of pulses induced solely by fast neutrons. The response matrix of the single-crystal diamond for fast neutrons was evaluated using Geant4, and applied to the energy deposition spectrum in the SCDD induced by fast neutrons. The results indicated the deduced neutron energy spectrum by the present method were consistent with the radiation transport calculation.

- [1] K. Mukai *et al.*, *Materials & Design* **253**, 113964 (2025).
- [2] T. Nagasaka *et al.*, *Nuclear Science and Technology Open Research* **2**, 56 (2024).
- [3] J.J. Shen, *Materials Science and Engineering: A* **915**, 147263 (2024).
- [4] M.I. Kobayashi *et al.*, *IEEE Trans. Instrum. Meas.* **73**, 6010808 (2024).

(M. Kobayashi)

Applied Superconductivity and Cryogenics (ASC) Unit

Highlight

The Applied Superconductivity and Cryogenics (ASC) Unit has conducted various research projects in fiscal year 2024 on applied superconductivity, including superconducting magnet technology, and cryogenics, such as those related to liquid hydrogen. Here are some of the highlights:

For the development of large-current High-Temperature Superconducting (HTS) conductors, experiments were conducted on REBCO-stacked conductor samples in collaboration with Helical Fusion, a startup company. A numerical analysis of the non-uniform current distribution has continued for the stacked conductor, STARS, which has been developed at NIFS for over fifteen years with continuous innovation.

For the HTS magnet, inspection of winding conductors is also a key technology. We employ a method of rotating magnetization for non-destructive, non-contact inspection of areas of critical current degradation in conductors made of laminated REBCO tapes. The details are described in the following section.

Low-Temperature Superconducting (LTS) conductors have also been developed to an advanced stage. A detailed description of a mechanically reinforced niobium-tin conductor is given in the following section. We are also proceeding with a collaboration with the National Institute for Materials Science (NIMS) to produce an Nb₃Al ultra-fine wire with a diameter of 50 μm. We have successfully made a single-cored wire of over 6 km in length without breakage or abnormal deformation during processing.

Liquid hydrogen cooling is the focus of a new approach for superconducting magnet technology. A series of experiments using liquid hydrogen for cooling a superconducting magnet has been conducted at the JAXA site in Noshiro, Akita Prefecture, in collaboration with Kyoto University and the Japan Aerospace Exploration Agency (JAXA), utilizing a liquid hydrogen testing facility. A cryostable condition was observed and investigated, where a normal-conducting transition does not lead to a thermal runaway due to the excellent cooling properties of liquid hydrogen.

A deep learning model has been developed and applied to predict the cooling characteristics of the LHD helical coils based on measurement data accumulated over the long years of LHD operation. We have succeeded in highly accurate predictions of temperature changes that occur when the helical coils are energized.

When cooling cryogenic equipment components, such as pipes and tanks, using a saturated liquid, like liquid nitrogen, it is essential to minimize the pre-cooling time to reduce refrigerant consumption. In past studies, it has been experimentally demonstrated that coating heat-transfer surfaces with low thermal conductivity material, such as resin, promotes boiling heat transfer and reduces the pre-cooling time. This is called the “insulation layer paradox”. We conducted rapid cooling experiments using copper plates coated with various fluoropolymers to elucidate the mechanism of heat transfer enhancement.

(N. Yanagi)

HIP process on mechanical strength improvement for internal matrix reinforced Nb₃Sn superconducting wire

The high mechanical strength of superconducting wires such as Niobium-Tin (Nb₃Sn) and HTS is an extremely urgent research issue for future fusion magnets with high magnetic fields. We previously demonstrated the high mechanical strength of conventional bronze-processed Nb₃Sn wire by an innovative internal matrix reinforcement method using Cu-Sn-X ternary alloy as the wire matrix component, as shown in Fig. 1. The third additional element, “X”, remained homogeneously distributed within the wire matrix after Nb₃Sn phase synthesis. It contributed to forming a high-mechanical-strength (Cu, X) solid solution as a reinforcement material. For further improvement in mechanical strength, the effect of Hot Isostatic Pressing (HIP) treatment after the Nb₃Sn phase synthesis was investigated. The HIP treatment was performed at a temperature of 650°C for two hours under a high pressure of 200 MPa in an argon atmosphere using the NIFS-HIP facility. Transport critical current (*I_c*) measurements under uniaxial tensile deformation were carried out using a special *I_c* probe with a uniaxial tensile deformation mechanism at the Institute for Materials Research, Tohoku University. Comparisons of the major mechanical strength properties in internal matrix-reinforced Nb₃Sn wire samples using Cu-Sn-In ternary alloys were investigated with and without HIP processing. HIP treatment improved all the major mechanical strength parameters. This was caused by the removal of Kirkendall voids in the wire matrix, which formed due to volume changes in the matrix during the Nb₃Sn synthesis heat treatment. On the other hand, the degree of improvement in mechanical strength achieved by the HIP treatment varied significantly depending on the composition of the ternary alloy used as the wire matrix. In the future, the primary reason for this dependence will be clarified through microstructural observation and crystallographic analyses.

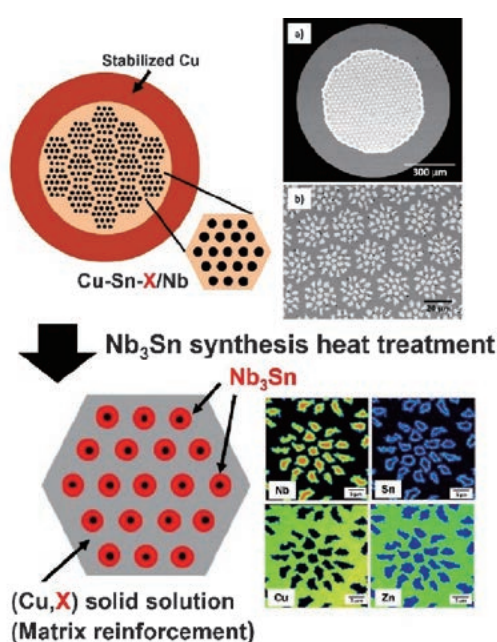


Fig. 1 Illustrative image of the “internal matrix reinforcement method” for producing niobium-tin wire via the solid solution hardening mechanism.

(Y. Hishinuma)

Non-destructive detection of degraded regions in stacked HTS conductors using rotating magnetization method

The development of superconducting magnets for fusion reactors requires conductors that can carry large currents stably and reliably. High-temperature superconductors (HTS), such as REBCO tapes, are promising candidates due to their high critical current density under high magnetic fields. However, performance degradation can occur during the fabrication of HTS-based multilayer high-current conductors, which makes the development of non-destructive evaluation techniques essential. In multilayer REBCO structures, even localized reductions in critical current can significantly impact overall performance, underscoring the need for internal diagnostic methods. In this study, we applied a non-destructive technique based on the rotating magnetization method, which evaluated the conductor’s magnetic response under an externally applied rotating magnetic field. A test sample consisting of ten stacked REBCO tapes was fabricated, with a localized degradation site intentionally introduced. The degraded region was identified through both experimental measurements and numerical analysis, demonstrating the feasibility and reliability of the proposed method.

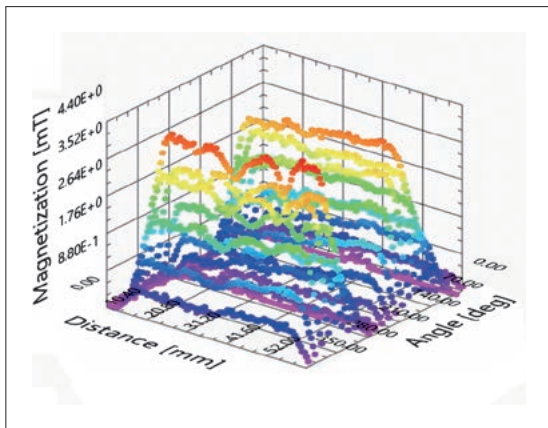


Fig. 2 Measured magnetization signal on the HTS conductor sample obtained from the rotating magnetization test.

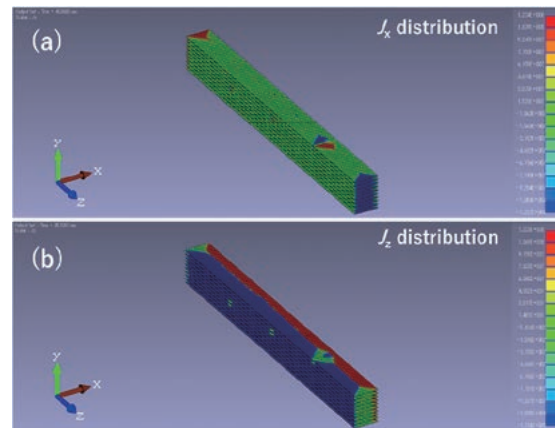


Fig. 3 In-plane current distribution in the HTS conductor sample obtained by a finite element analysis: (a) across the tape width; (b) along the longitudinal direction.

(Y. Onodera)

